ARTICLES

Ultrafast Excited-State Dynamics Preceding a Ligand Trans−Cis Isomerization of *fac*-[Re(Cl)(CO)$_3$(*t*-4-styrylpyridine)$_2$] and *fac*-[Re(*t*-4-styrylpyridine)(CO)$_3$(2,2′-bipyridine)]$^+$

Michael Busby,[†] Pavel Matousek,[‡] Michael Towrie,[‡] and Antonín Vlček, Jr.*[,†]

Department of Chemistry and Centre for Materials Research, Queen Mary, University of London, Mile End Road, London E1 4NS, United Kingdom, and Central Laser Facility, CCLRC Rutherford Appleton Laboratory, Chilton, Didcot, Oxfordshire OX11 0QX, United Kingdom

Received: November 17, 2004; In Final Form: January 24, 2005

UV−vis absorption and resonance Raman spectra of the complexes *fac*-[Re(Cl)(CO)$_3$(stpy)$_2$] and *fac*-[Re(stpy)(CO)$_3$(bpy)]$^+$ (stpy = *t*-4-styrylpyridine, bpy = 2,2′-bipyridine) show that their lowest absorption bands are dominated by stpy-localized intraligand (IL) $\pi\pi^*$ transitions. For the latter complex a Re → bpy transition contributes to the low-energy part of the absorption band. Optical population of the ^{1}IL excited state of *fac*-[Re(Cl)(CO)$_3$(stpy)$_2$] is followed by an intersystem crossing (≤0.9 ps) to an ^{3}IL state with the original planar trans geometry of the stpy ligand. This state undergoes a ∼90° rotation around the stpy C═C bond with a 11 ps time constant. An electronically excited species with an approximately perpendicular orientation of the phenyl and pyridine rings of the stpy ligand is formed. Conversion to the ground state and isomerization occurs in the nanosecond range. Intraligand excited states of *fac*-[Re(stpy)(CO)$_3$(bpy)]$^+$ show the same behavior. Moreover, it was found that the planar reactive ^{3}IL excited state is rapidly and efficiently populated after optical excitation into the Re → bpy ^{1}MLCT excited state. A ^{1}MLCT → ^{3}MLCT intersystem crossing takes place first with a time constant of 0.23 ps followed by an intramolecular energy transfer from the Re$^{\mathrm{I}}$(CO)$_3$(bpy) chromophore to a stpy-localized ^{3}IL state with a 3.5 ps time constant. The fast rate ensures complete conversion. Coordination of the stpy ligand to the Re$^{\mathrm{I}}$ center thus switches the ligand trans−cis isomerization mechanism from singlet to triplet (intramolecular sensitization) and, in the case of *fac*-[Re(stpy)(CO)$_3$(bpy)]$^+$, opens an indirect pathway for population of the reactive ^{3}IL excited state via MLCT states.

Introduction

Photochemical trans−cis isomerization of an olefinic C═C bond is one of the fundamental photochemical processes. Its investigations by ultrafast spectroscopic techniques[1−5] and quantum chemical calculations[6] keep revealing important new insights into the nature of the excited states involved, their relaxation and dynamic couplings, dynamics of barrier crossing, and the isomerization itself. Besides its fundamental interest, photoisomerization is responsible for the capture of optical information by retinal[7−10] in the processes of vision and for functioning of important biomolecules such as the photoactive yellow protein[11] or rhodopsin.[12] It can be envisaged that photoisomerization can perform similar functions in man-made molecular devices, where photoisomerizable molecules could serve as switches or memory units.[12]

Over many years stilbene has been the model photoisomerizable molecule.[13] The generally accepted mechanistic picture[6] originates in the work by Saltiel[14] and Orlandi.[15] The reaction occurs on the potential-energy surface of the optically populated $^1\pi\pi^*$ state, overcoming a small energy barrier to produce an intermediate singlet excited state with a perpendicular geometry of the phenyl rings. Nonradiative transition to the maximum on the ground-state potential-energy surface follows through a conical intersection. The molecule then either rotates further 90° to the cis isomer or twists back to the trans configuration. A lifetime of 90 ps has been determined[16] for the $^1\pi\pi^*$ state in *n*-hexane at room temperature. A similar mechanism operates on the triplet potential-energy surface. However, intersystem crossing from $^1\pi\pi^*$ is not competitive with isomerization, and the reactive $^3\pi\pi^*$ state can be populated only by using triplet sensitizers.[17−19] The efficiency of intersystem crossing to the $^3\pi\pi^*$ state and the relative contribution of the triplet mechanism to the trans−cis isomerization can also be enhanced by a heavy-atom effect of bromo or chloro substituents in 4-halogenated stilbenes.[20] The perpendicular triplet state of stilbene is nearly isoenergetic with the perpendicular form of the ground state.[6,15] Nevertheless, because of its spin-forbidden character, the intersystem crossing to the ground state is rather slow, ca. 60 ns.[17,21]

Introduction of a nitrogen atom into one or two of the stilbene aromatic rings yields styrylpyridine or 1,2-bis-pyridylethylene, respectively. These compounds undergo the same trans−cis photoisomerization as stilbene, again following the singlet and triplet mechanisms.[22,23] Moreover, they can also act as ligands, binding to transition-metal atoms via their pyridyl rings. Photoisomerization reactivity of stilbene-like molecules is

* To whom correspondence should be addressed.
[†] University of London.
[‡] CCLRC Rutherford Appleton Laboratory.

10.1021/jp044753+ CCC: $30.25
Published on Web 03/11/2005

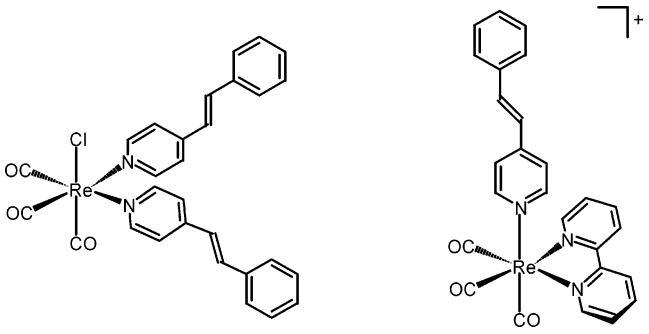

Figure 1. Schematic structures of *fac*-[Re(Cl)(CO)$_3$(stpy)$_2$] (left) and *fac*-[Re(stpy)(CO)$_3$(bpy)]$^+$ (right).

generally retained upon coordination to transition-metal complexes. A relatively slow ($\sim 10^6$ s^{-1}) trans−cis isomerization of the stilbene unit in [Re(stilbene-amido-pyridine)(CO)$_3$(bpy)]$^+$ (bpy = 2,2′-bipyridine) follows optical excitation of the Re → bpy metal to ligand charge transfer (MLCT) transition.[24] Efficient ($\phi = 0.54$ at 366 nm) isomerization was found[19] in *fac*-[Re(Cl)(CO)$_3$(stpy)$_2$], where the 4-styrylpyridine (stpy) ligand is directly coordinated to the Re atom. Less efficient isomerization was reported[25] for *fac*-[Re(stpy)(CO)$_3$(NN)]$^+$ (NN = bpy or phen = 1,10-phenanthroline), while quantum yields ≈ 0.2 were found[26,27] in complexes with 1,2-bis(4-pyridyl)-ethylene (bpe), *fac*-[Re(bpe)(CO)$_3$(NN)]$^+$. Bridging pyridyl−ethylene-type ligands can also link two Re(CO)$_3$(NN) units, leading to photoactive polynuclear[28−30] complexes. Trans−cis isomerization of complexes containing pyridyl−ethylene ligands coordinated to a Re(CO)$_3$(NN) unit is accompanied by emergence of a strong emission, a function which could possibly be utilized in molecular devices.[31,32]

Coordination of stilbene-like isomerizable molecules to transition metals presents new opportunities and brings up further mechanistic questions: (i) Is the singlet isomerization mechanism still operational or does metal coordination steer the reaction to the triplet potential-energy surface? (ii) What is the nature of the photoreactive state(s) and intermediates involved? (iii) Can MLCT excitation to a stilbene-type ligand induce its isomerization? (iv) Is it possible to trigger isomerization of a stilbene-type ligand by exciting a MLCT transition directed to a polypyridine ligand simultaneously present in the coordination sphere? The latter question is especially important. Population of reactive intraligand (IL) $\pi\pi^*$ excited states upon Re → NN MLCT excitation of *fac*-[Re(L)(CO)$_3$(NN)]$^+$ complexes (L = photoisomerizing stilbene-type ligand) was often assumed[25,28,31] to occur with modest rates but never proven directly. Such an intramolecular energy transfer, if sufficiently fast, would provide an alternative way to trigger trans−cis isomerization using relatively low-energy light, with possible device applications.

Herein, we studied complexes *fac*-[Re(Cl)(CO)$_3$(stpy)$_2$] and *fac*-[Re(stpy)(CO)$_3$(bpy)]$^+$ (Figure 1), which are further abbreviated as Re(stpy)$_2$ and Re(stpy)(bpy), respectively. A combination of stationary and ultrafast time-resolved spectroscopic techniques was employed with the aim of understanding the nature and dynamics of the first steps leading to isomerization of metal-bound stilbene-type ligands. It is shown that stpy-localized ^{3}IL excited states are populated very rapidly and efficiently, following optical excitation to either ^{1}IL or Re → bpy ^{1}MLCT states. Intramolecular energy transfer from an ^{3}MLCT to ^{3}IL state is directly observed for the first time. Moreover, a picosecond structural reorganization of the stpy ^{3}IL state was clearly demonstrated and attributed to a trans → perpendicular twist around the C=C bond.

Experimental Section

Materials. All starting chemicals were obtained from Aldrich and used as received. Solvents of spectroscopic quality were used. The stpy ligand and the complexes were prepared according to modified literature procedures.

***trans*-4-Styrylpyridine (stpy).**[33] An equimolar mixture of benzaldehyde (10.61 g, 0.1 mol) and 4-picoline (9.31 g, 0.1 mol) was refluxed in 200 mL of acetic anhydride for 18 h. The mixture was allowed to cool, quenched with 60 mL of water, and made pH 8−9 with 30% NaOH. The brown solid was separated via vacuum filtration, washed with water, and dried over silica under reduced pressure for 24 h. The crude compound was twice sublimed at 135 °C, 0.1 mmHg, and then recrystallized from methanol, producing white needles: 61% yield.

^{1}H NMR (CD$_3$CN, 270 MHz): δ 7.17 (1H, d, $J = 16.2$, ethylenic CH), 7.38 (4H, m), 7.47 (2H, d, $J = 8.1$, aromatic CH), 7.51 (2H, d, $J = 8.1$, aromatic CH), 8.54 (2H, d, $J = 5.4$, aromatic CH).

fac-[Re(Cl)(stpy)$_2$(CO)$_3$].[19]

[Re(Cl)(CO)$_5$] (0.52 g, 1.44 mmol) and stpy (0.58 g, 3.2 mmol) were refluxed in dry toluene for 12 h. The solution was cooled, and the volume was reduced to a minimum. The precipitate was filtered under suction and then washed with pet spirits (60−80 °C) to remove any excess free ligand: 92% yield.

FT IR (CH$_2$Cl$_2$): ν_{CO} = 2024(s), 1920(m), 1886(m) cm^{-1}.

^{1}H NMR (CDCl$_3$, 270 MHz): δ 6.98 (2H, d, $J = 16.3$, ethylenic CH), 7.39 (12H, m, CH), 7.52 (4H, d, $J = 8.1$, aromatic CH), 8.67 (4H, d, $J = 6.7$, aromatic CH).

fac-[Re(stpy)(CO)$_3$(bpy)]PF$_6$.[25]

fac-[Re(OTf)(CO)$_3$(bpy)][34] (1.18 g, 2.06 mmol) and stpy (0.41 g, 2.26 mmol) were refluxed in 30 mL of dry THF for 12 h. The mixture was filtered hot, and the solvent was then removed in vacuo. The solid was dissolved in 30 mL of methanol, and a saturated solution of methanol containing 1 g of NH_4PF_6 was added to form a precipitate, which was then filtered and repeatedly recrystallized from methanol: 63% yield.

FT-IR (CH$_2$Cl$_2$): ν_{CO} = 2035(s), 1934 (br) cm^{-1}.

^{1}H NMR (CD$_3$CN, 270 MHz): δ 7.05 (1H, d, $J = 16.2$, ethylenic CH), 7.39 (6H, m, CH), 7.56 (2H, d, $J = 7.9$, aromatic CH), 7.79 (2H, dd, $J = 7.9$, aromatic CH), 8.13 (2H, d, $J = 6.7$, aromatic CH), 8.26 (2H, dd, $J = 7.9$, aromatic CH), 8.36 (2H, d, $J = 8.2$, aromatic CH), 9.23 (2H, d, $J = 5.4$, aromatic CH).

^{13}C NMR (CD$_3$CN, 67.9 MHz): δ 124.23, 124.87, 125.79, 128.55, 129.85, 130.22, 130.67, 136.69, 137.98, 142.19, 149.43, 152.93, 154.90, 156.83, 196.89 (CO).

Spectroscopic Techniques. Ground-state resonance Raman spectra were obtained using a Coherent Innova 90-5 UV argon-ion laser with a power output of ca. 50 mW at 457.9 nm and 30 mW at 351.1 nm. The Raman spectra were recorded using 2 mm quartz flow tubes, and the scattered light was collected at 90° from the excitation beam passed through a Spex Triplemate 187 Series monochromator and dispersed across a Princeton Instruments LN/CCD-1024 CCD camera. Spectra were calibrated and solvent bands subtracted using CSMA CCD Spectrometric Multichannel Analysis Software, version 2.4a, Princeton Instruments Inc.

Time-resolved UV−vis absorption spectra, TA, were measured using the experimental setup at the van't Hoff Institute for Molecular Sciences, University of Amsterdam.[35] A ~130 fs, 390 nm pump pulse was generated by frequency doubling of the Ti:Sapphire laser output. White-light continuum probe pulses were generated by focusing the 780 nm fundamental in a sapphire plate. Some TA spectra were obtained using the

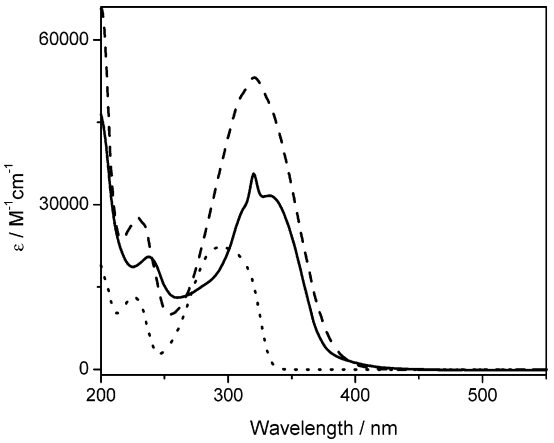

Figure 2. UV−vis absorption spectra of stpy in acetonitrile (····), [Re(Cl)(CO)$_3$(stpy)$_2$] in CH_2Cl_2 (- - -), and [Re(stpy)(CO)$_3$(bpy)]$^+$ in acetonitrile (—).

equipment at the Rutherford Appleton Laboratory,[36] using ∼200 fs, 400 nm pulses and a white-light continuum generated with 800 nm fundamental in H_2O flowing through a quartz cell.

Time-resolved IR (TRIR) and Kerr-gate resonance Raman (TR^3) experiments used the equipment and procedures described in detail previously.[36−42] In short, the sample solution was excited (pumped) at 400 nm using frequency-doubled pulses from a Ti:sapphire laser of ∼150 fs duration (fwhm) for TRIR, while pulses of 1−2 ps duration were used for Raman studies. TRIR spectra were probed with IR (∼150 fs) pulses obtained by difference-frequency generation. The IR probe pulses cover a spectral range ca. 200 cm^{-1} wide and are tunable from 1000 to 5000 cm^{-1} (i.e., 2−10 μm). Kerr-gate TR^3 spectra were probed at 475 nm using an OPA. Kerr gate was employed to remove all long-lived emission from the Raman signal. TR^3 spectra were corrected for the Raman signal due to the solvent and the solute ground state by subtracting the spectra obtained at negative time delays (−50, −20 ps) and subtracting any weak residual fluorescence emission that passed through the Kerr gate. The sample solutions for picosecond TR^3 and TRIR experiments were flowed as a 0.5 mm open jet and through a 0.5 mm CaF_2 raster-scanned cell, respectively.

The spectral bands observed in TRIR spectra were fitted by Lorentzian functions to determine accurately their center positions, widths, and areas. All spectral fitting procedures were performed using Microcal Origin 7 software.

Results

UV−Vis Absorption and Resonance Raman Spectroscopy. The UV−vis spectrum of the free stpy ligand (Figure 2) shows a strong absorption at 295 nm that was assigned[43] to almost degenerate $^1\pi\pi^*$ and $^1n\pi^*$ transitions. For Re(stpy)$_2$ there is a strong absorption band at 320 nm (ϵ = 53 100 M^{-1} cm^{-1}) which resembles that of protonated stpyH$^+$.[19] This band has been assigned, through low-temperature studies, to an intraligand (IL) $\pi\pi^*$ transition.[19] Re(stpy)(bpy) exhibits a similar absorption spectrum with a broad band centered at ∼332 nm. Its molar absorptivity (∼31 650 M^{-1} cm^{-1}) is by ∼5100 M^{-1} cm^{-1} higher than one-half of that of the IL band of Re(stpy)$_2$. This indicates that the band arises from a stpy-localized IL transition with contributions from MLCT and bpy-localized IL transitions, the latter being manifested by the spike at 320 nm. A weak tail extending to about 420 nm is attributed to a Re → bpy MLCT transition, based on comparison with spectra of [Re(L)(CO)$_3$(bpy)]$^+$ complexes, where L is a pyridine-type ligand.[34,44]

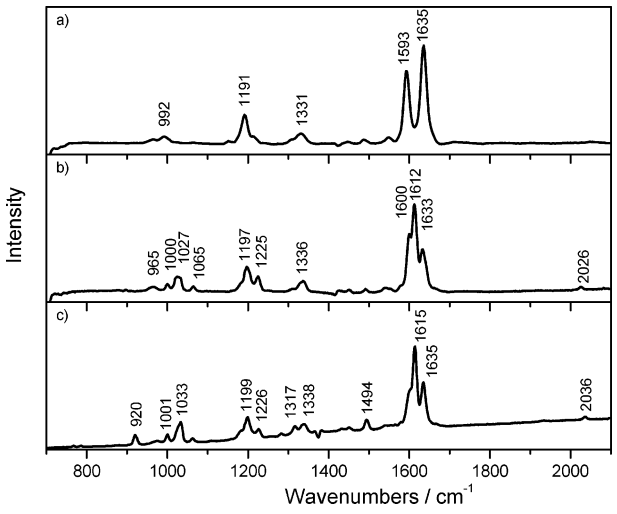

Figure 3. Resonance Raman spectra of (a) stpy in CH_2Cl_2, excited at 351.1 nm, (b) [Re(Cl)(CO)$_3$(stpy)$_2$] in CH_2Cl_2, excited at 457.9 nm, and (c) [Re(stpy)(CO)$_3$(bpy)]$^+$ in acetonitrile, excited at 457.9 nm. Solvent bands have been subtracted.

These spectral assignments are confirmed by (pre)resonance Raman spectra shown in Figure 3. The spectrum of free stpy, excited at 351.1 nm, shows strongly enhanced bands at 1593 (s) and 1635(vs) cm^{-1} and weaker ones at 1311, 1191, and 992 cm^{-1}. The similarity with the spectrum of stilbene allows us to assign the 1635 cm^{-1} band to stretching vibration of the ethylenic C═C bond, coupled to the ethylenic C−H symmetric in-plane bend, and the 1593 cm^{-1} band to the ring CC stretches, with minor contributions from the ethylenic C═C and C−Ph/py stretches.[45] The preresonance Raman spectrum of Re(stpy)$_2$ is similar to that of the free ligand. Three bands at 1600(s), 1612(vs), and 1632(m) cm^{-1} are seen. On the basis of their similarity to the stpy 1593−1635 cm^{-1} doublet, they are thought to originate in vibrations with a significant ν(C═C) character. The weakness of the ν(CO) A′(1) band at 2026 cm^{-1} effectively rules out any significant contribution of a Re → stpy MLCT transition to the resonant enhancement. (Preresonance with MLCT transitions is known[46,47] to strongly enhance Raman bands due to the in-phase symmetric CO vibrations, as seen, for example, in the rR spectrum[44] of [Re(Cl)(CO)$_3$(4-benzoylpyridine)$_2$].) It can be concluded that the predominant resonant electronic transition, which is also responsible for the 320 nm absorption band, has a $\pi\pi^*$ IL character, very similar to that of free stpy.

The rR spectrum of Re(stpy)(bpy) is very similar to that of Re(stpy)$_2$. The three vibrations with ν(C═C) character are again seen at 1601(sh), 1615(vs), and 1635(m) cm^{-1} together with a band at 1226(w) cm^{-1}. The A′(1) ν(CO) metal−carbonyl mode is observed at 2036 cm^{-1}, though its resonant enhancement is minute compared to other bands, indicating that the Raman intensity enhancement originates predominantly in the stpy-localized IL $\pi\pi^*$ transition. However, the presence of a weak band at 1494 cm^{-1}, which corresponds to a bpy-localized vibration,[48,49] indicates a small contribution from a Re → bpy MLCT transition.

Ultrafast Excited-State Dynamics. *Transient Visible Absorption Spectroscopy (TA).* The TA spectra of free stpy show a broad intense band at ca. 515 nm, Figure 4a. Its decay is accompanied by a small shift of the band maximum to shorter wavelengths caused by vibrational cooling[50] and appearance of a shoulder at ca. 450 nm. The decay kinetics are biexponential with time constants of 1.7 ± 0.1 (84%) and 8.6 ± 0.4 ps (16%) at 510 nm (Figure 5a) and 3.1 ± 0.5 (46%) and 14.4 ± 10.0 ps

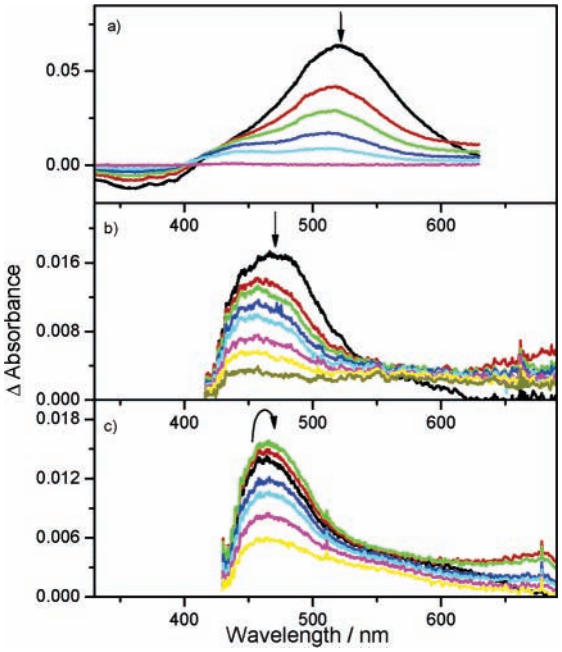

Figure 4. Difference transient absorption spectra of (a) stpy in acetonitrile, measured after 276 nm excitation (spectra shown at 2 (black), 3 (red), 4 (green), 6 (dark blue), 10 (light blue), and 50 (pink) ps), (b) $[Re(Cl)(CO)_3(stpy)_2]$ in CH_2Cl_2, measured after 400 nm excitation (spectra shown at 0 (black), 1 (red), 2 (green), 4 (dark blue), 6 (light blue), 12 (red), 20 (yellow), and 500 (brown) ps), and (c) $[Re(stpy)(CO)_3(bpy)]^+$ in acetonitrile, measured after 400 nm excitation (spectra shown at 2 (black), 3 (red), 6 (green), 16 (dark blue), 20 (light blue), 30 (pink), and 500 (yellow) ps). Chirp distorts early spectral timing between 0 and 2 ps.

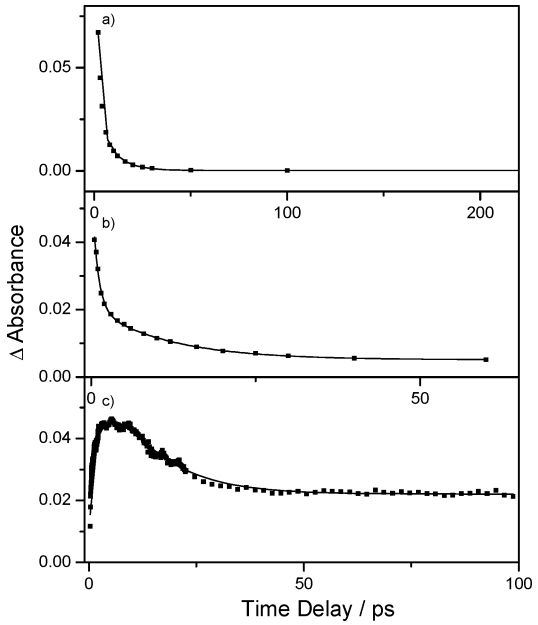

Figure 5. Kinetic absorbance profiles and fits of transient absorption of (a) stpy at 510 nm in acetonitrile, excited at 276 nm, (b) $[Re(Cl)(CO)_3(stpy)_2]$ at 470 nm in CH_2Cl_2, excited at 400 nm, and (c) $[Re(stpy)(CO)_3(bpy)]^+$ at 470 nm in acetonitrile, excited at 400 nm. Absorbance values were measured as a 10 pixel average around the probe wavelength. The corresponding TA spectra are shown in Figure 4.

(53%) at 462 nm. The band at 515 nm resembles the TA band seen for *t*-stilbene at 585 nm[16,50] and is attributed to a $^1\pi\pi^*$ state. The 450 nm shoulder is tentatively assigned to a $^1n\pi^*$ state. The short decay component is similar to the fluorescence lifetime of 2.6 ps measured in *n*-hexane.[43]

The TA spectrum of $Re(stpy)_2$ (Figure 4b) is distinctly different from that of free stpy. An intense, broad transient band appears within the instrument time resolution (<500 fs) at wavelengths shorter than ca. 550 nm. The maximum at ca.470 nm is only apparent, resulting from overlapping negative absorption due to a bleached ground state at shorter wavelengths. This band rapidly decays in intensity, narrows, and blue shifts during the first few picoseconds. Further decay occurs between 2 and 40 ps, leaving a broad, weak featureless signal that extends from 430 to 700 nm and does not change during the 1 ns time interval investigated. The decay kinetics determined at 470 nm is biexponential: 0.9 ± 0.1 (64%) and 11.4 ± 1.3 ps (27%) with a time-independent term (9%) that reflects the long-lived ($\gg$1 ns) signal, Figure 5b. Similar biexponential decay kinetics are seen in the region of a weak absorbance between 620 and 700 nm. The large relative weight of the 0.9 ps kinetic component indicates that it corresponds to excited-state decay of the optically prepared ^1IL_t excited state, as opposed to its vibrational cooling. (The subscript "t" denotes the original trans geometry of the stpy C=C bond.) The resulting spectrum is assigned to a triplet ^3IL_t state of a $\pi\pi^*$ origin because of its similarity with the excited-state spectra of *t*-stilbene,[17,18] whose $^3\pi\pi^*$ state absorbs only in the near UV region, while the corresponding singlet state shows a strong band in the visible for both stilbene[17,18] and free stpy (Figure 4a). The 0.9 ps step is thus assigned as a $^1IL_t \rightarrow {}^3IL_t$ intersystem crossing. The ^3IL_t state then undergoes a further 11.4 ps process which yields a long-lived, weakly absorbing species. TA spectra provide no information on its character. Finally, it should be noted that the TA spectra show no evidence of a Re $\rightarrow$ stpy MLCT state, which would be expected to show a sharp strong absorbance at ca. 490 nm and a weaker absorbance at ca. 690 nm, based on the UV−vis spectrum of the stilbene radical anion.[51]

The TA spectrum of Re(stpy)(bpy) is shown in Figure 4c. A weak transient with an apparent maximum at 460−470 nm grows with biexponential (0.23 ± 0.02 and 3.5 ± 0.3 ps) kinetics (Figure 5c), reaching its maximum intensity by ~6 ps. Its shape and intensity closely resemble that of $Re(stpy)_2$ at time delays $\geq$2 ps and is thus attributed to the same ^3IL_t state. The band subsequently decays with a 11.7 ± 0.8 ps lifetime into a weak broad signal that covers most of the visible spectral region and shows no further temporal evolution between 100 and 1000 ps.

Time-Resolved Resonance Raman Spectroscopy, TR^3. TR^3 spectra of free stpy (Figure 6a) were obtained after 300 nm pumping using a 475 nm probe that is directed into the blue side of the excited-state absorption band (Figure 4a). Lorentzian fitting of the weak signal obtained at a 5 ps delay has identified TR^3 peaks at 1576 ± 2 (s), 1280 ± 4 (m), 1164 ± 2 (s), 986 ± 5 (w), and 846 ± 4 (w) cm^{-1}. On the basis of the comparison with TR^3 spectra of the $^1\pi\pi^*$ and $^3\pi\pi^*$ states of *t*-stilbene,[18,52] these bands are tentatively assigned to ν(CC), in-plane δ(CH), ring δ(CC) + in-plane $\delta(C_{ring}H)$, in-plane $\delta(C_{ring}H)$, and ν(CC)+δ(CCC) modes, respectively. The Raman bands decay with a lifetime (ca. 4 ps for the 1576 cm^{-1} band) that approximately corresponds to that of the TA band. Concomitantly, they undergo a small dynamic shift to higher wavenumbers, caused by vibrational cooling.[52,53]

For $Re(stpy)_2$ TR^3 spectra (Figure 6b) were measured in CH_2Cl_2 at 400 nm with the probe beam directed into the maximum of the TA band at 475 nm. Very weak broad bands were acquired that have been fitted to Lorentzians at 1521 ± 1.1 (s), 1251 ± 4.0 (m), and 1022 ± 5.2 (w) cm^{-1}, measured in the 20 ps spectrum. As discussed for the TA spectra, the resonant transition in the TR^3 spectra originates in an ^3IL_t state. This is

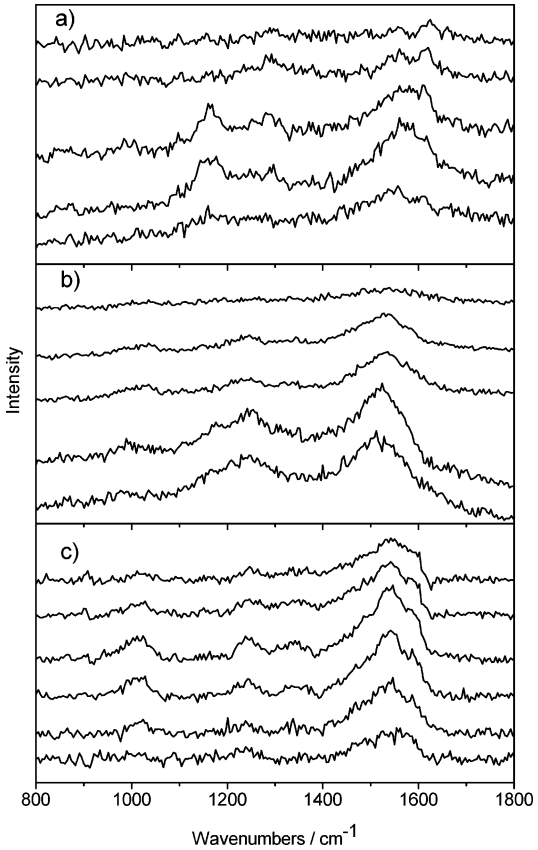

Figure 6. Kerr-gate time-resolved resonance Raman spectra of (a) stpy in CH_2Cl_2, probed with 475 nm laser pulses at 1, 3, 5, 20, and 500 ps after a 300 nm excitation, (b) $[Re(Cl)(CO)_3(stpy)_2]$ in CH_2Cl_2, probed with 475 nm laser pulses, at 0, 2, 6, 10, and 50 ps after 400 nm excitation, and (c) $[Re(stpy)(CO)_3(bpy)]^+$ in acetonitrile, probed with 475 nm laser pulses at 0, 2, 5, 8, 30, and 100 ps after 400 nm excitation. Spectra evolve from bottom to top.

now confirmed by the presence of Raman bands that resemble those of the $\pi\pi^*$ state of free stpy. Fitting the time evolution of the area of the 1521 cm^{-1} band from 2 ps onward reproduces the ~11 ps decay measured in the TA.

Re(stpy)(bpy) was excited at 400 nm and its TR^3 spectra (Figure 6c) probed at 475 nm. As in the TA spectra, the TR^3 peaks exhibit a fast rise with a time constant of 3.2 ± 0.9 ps. The TR^3 bands are broad with Lorentzian-fitted maxima at 1535 ± 1.3 (s), 1343 ± 13.4 (m), 1244 ± 3.5 (m), and 1015 ± 3.6 (m) cm^{-1}, measured at 30 ps. The bands are at comparable positions to those seen for $Re(stpy)_2$ and are hence assigned to a stpy-localized ^3IL_t state. It is obvious that this state is formed from another precursor state that has neither strong absorption in the visible region nor strongly resonance-enhanced Raman bands. A Re → bpy MLCT is a likely candidate for the precursor state. The ^3IL TR^3 bands decay completely with a lifetime estimated as 20 ± 9 ps.

Time-Resolved Infrared Spectroscopy (TRIR). TRIR spectra were investigated in the spectral regions of ν(CO) and stpy-localized vibrations following excitation at 400 nm. Spectra measured at the earliest time delays are complicated by coherence effects which usually subside at 1−3 ps. The TRIR spectra in the ν(CO) region of both complexes are shown in Figure 7, while Figures 8 and 9 provide detailed views of the high-frequency region.

The spectrum of $Re(stpy)_2$ measured 2 ps after 400 nm laser-pulse excitation shows bleached ground-state ν(CO) bands at 2024, 1917, and 1884 cm^{-1} and a transient consisting of a sharp

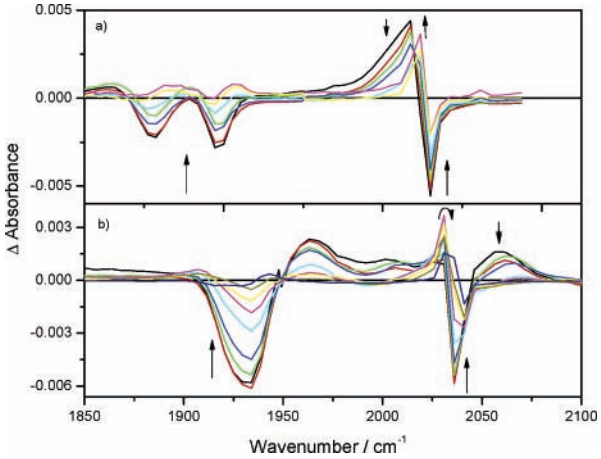

Figure 7. Difference time-resolved infrared spectra of (a) $[Re(Cl)(CO)_3(stpy)_2]$ in CH_2Cl_2 (spectra shown at 2 (black), 6 (red), 10 (green), 20 (dark blue), 50 (light blue), 100 (pink), and 1000 (yellow) ps) and (b) $[Re(stpy)(CO)_3(bpy)]^+$ in CH_2Cl_2 (spectra shown at 1 (black), 1.5 (red), 2 (green), 3 (dark blue), 6 (light blue), 10 (pink), 20 (yellow), 30 (brown), and 1000 (gray) ps). Both complexes are measured after 400 nm excitation. Experimental points are separated by 4−5 cm^{-1}.

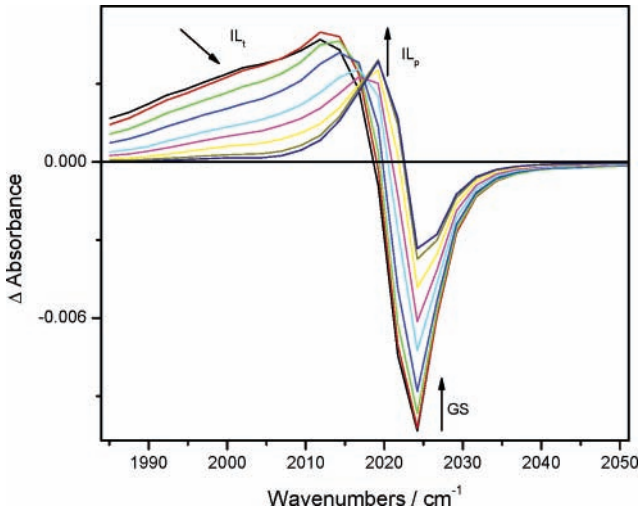

Figure 8. Difference time-resolved infrared spectra of $[Re(Cl)(CO)_3(stpy)_2]$ in CH_2Cl_2, measured after 400 nm excitation (spectra shown at 3 (black), 4 (red), 6 (green), 10 (dark blue), 20 (light blue), 30 (pink), 50 (yellow), 100 (brown), and 1000 (gray) ps). Experimental points are separated by ca. 2 cm^{-1}.

band at 2012 cm^{-1} and a weak, broad feature at ~1864 cm^{-1}, see Figures 7a and 8a. This IR spectral pattern is characteristic[54−57] of a $\pi\pi^*$ IL state, as seen, for example, for $[Re(4\text{-}Etpy)(CO)_3(dppz)]^+$ and similar complexes. TRIR spectra thus confirm the stpy-localized ^3IL_t character of the initially populated excited state of $Re(stpy)_2$, in full accordance with the TA and TR^3 evidence discussed above. The 2012 cm^{-1} band narrows and decreases in intensity between 2 and 40 ps, while another sharp band grows in at 2019 cm^{-1}. Concomitantly, the 1864 cm^{-1} feature shifts to higher wavenumbers, into the region of bleached ground-state absorption, giving rise to two apparent maxima at 1926 and 1894 cm^{-1}. An isosbestic point is seen at ~2017 cm^{-1}, indicating that the spectral change is caused by a clean conversion between two states. The new spectral pattern is again characteristic of an ^3IL state. As will be discussed below, we propose this state to have perpendicular orientation of the pyridine and phenyl rings. Hereafter it will be known as ^3IL_p. Once formed the 2019 cm^{-1} band stays constant from ca. 70 ps until the end of the time interval investigated, i.e., 1000 ps.

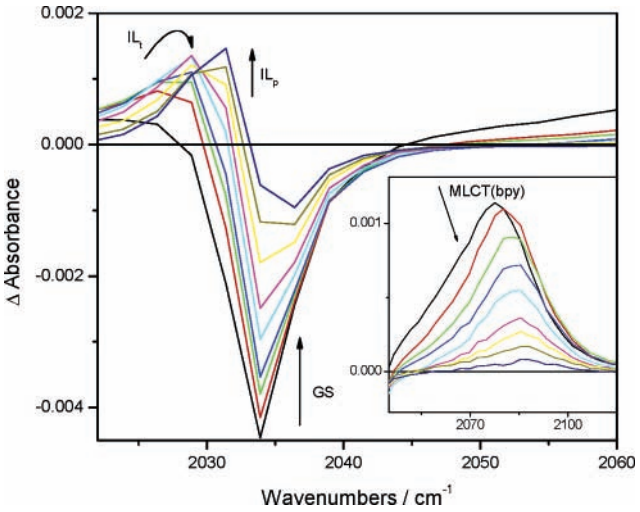

Figure 9. Difference time-resolved infrared spectra of $[Re(stpy)(CO)_3(bpy)]^+$ in acetonitrile, measured after excitation at 400 nm (spectra shown at 3 (black), 6 (red), 8 (green), 10 (dark blue), 15 (light blue), 20 (pink), 30 (yellow), 50 (brown), and 1000 (gray) ps). (Inset) MLCT(bpy) decay at 3 (black), 4 (red), 6 (green), 8 (dark blue), 10 (light blue), 15 (pink), 20 (yellow), 30 (brown), and 50 (gray) ps. Experimental points are separated by ca. 2 cm^{-1}.

Therefore, it is identified with the long-lived, weakly absorbing transient observed in TA. Quantitative analysis of the evolution of bleached ground-state bands is precluded by a strong overlap with the transient features. This overlap is higher for the ^3IL_p, as manifested by a decrease of the bleach during conversion.

The area of the 2012 cm^{-1} band, obtained by Lorentzian fitting, decays with a time constant of 11.8 ± 0.4 ps. The absorbance at 2019 cm^{-1} grows with a comparable rise time, 12 ± 3 ps. The decay constant of the 2012 cm^{-1} band is identical, within the instrumental precision, to the 11.4 ps component of the TA decay.

The assignment of the primary and secondary IR transients as ^3IL_t and ^3IL_p states with different orientations of the pyridine and phenyl rings of the stpy ligand implies that their ~12 ps conversion occurs as a ~90° rotation around the C═C bond. To confirm this assumption we studied this step in a PMMA film, where the rotation should be hindered by the medium rigidity. Indeed, the TRIR spectra of $Re(stpy)_2$ in PMMA show only the bleach at 2023 cm^{-1} and a broad ^3Il_t band at ca. 2012 cm^{-1}, which narrows between 1 and 40 ps due to cooling. It neither decays in intensity nor converts into any other band during the 1−2000 ps interval investigated.

TRIR spectra in the region of stpy ν(C═C) vibrations, 1580−1640 cm^{-1}, show a bleached ground-state band at 1612 cm^{-1} which becomes fully developed at 4−6 ps when the initial fast relaxation is completed. Overlapping broad background absorption and overall signal weakness prevents further analysis. No distinct transient IR feature was observed. Persistent bleaching of an IR band corresponding to a stpy-localized vibration supports the assignment of both transient features seen in the ν(CO) region to IL states.

The ν(CO) TRIR spectrum of Re(stpy)(bpy) (Figures 7b and 9) measured at 1 ps in CH_2Cl_2 shows the ground-state bleach bands at 1932 (A′(2) + A″) and 2034 cm^{-1} (A′(1)) and three transient bands at higher wavenumbers: 1963, 1995, and 2061 cm^{-1}. Such a spectral pattern is characteristic of a Re → bpy ^{3}MLCT excited state, as observed for $[Re(4\text{-Et-pyridine})(CO)_3(bpy)]^+$ and other complexes.[44,54,55,57−61] These spectral features essentially disappear within the first 6−10 ps. Concurrent with this fast decay the MLCT A′(1) 2061 cm^{-1} band undergoes a slight narrowing and upward shift to 2074 cm^{-1} with a time constant estimated as 4 ps. Such a behavior is typical for vibrational cooling.[61,62] In acetonitrile the A′(1) bleach and excited-state bands are seen at 2034 and 2076 cm^{-1}, respectively. Vibrational cooling shifts the latter band to 2085 cm^{-1} with a 3−4 ps time constant. The larger overall shift of the A′(1) band upon excitation in acetonitrile (+51 cm^{-1}) than in CH_2Cl_2 (+40 cm^{-1}) is caused by the higher polarity of the former solvent, which favors a larger shift of electron density from $Re(CO)_3$ to bpy. This solvent effect further supports the assignment of the early TRIR spectral pattern seen for Re(bpy)(stpy) to a ^{3}MLCT(bpy) state. Vibrational cooling severely affects the decay dynamics of the A′(1) MLCT band. This is manifested by the increase of the decay constant from ca. 2.4 to 8.9 ps with increasing the probe wavenumber across the A′(1) MLCT band. The band area, determined by Lorentzian fitting, decays with a time constant of 6.6 ± 1.7 ps in CH_2Cl_2. Similar decay dynamics were estimated in the region of the 1963 cm^{-1} band. Considering interfering effects of vibrational cooling, the decay of the ^{3}MLCT TRIR pattern can be identified with the 3.5 ps rise kinetics of the TA and TR^3 signals.

Decay of the ^{3}MLCT bands is accompanied by growth of a sharp transient band at 2027 cm^{-1} and a broad absorption between 1910 and 1960 cm^{-1}. The latter strongly overlaps with the A′(2) + A″ negative bleach bands, nearly canceling absorption in this spectral region. This secondary transient IR spectrum is characteristic of an IL excited state. It closely resembles the initial IR spectral pattern seen for $Re(stpy)_2$. Hence, it is attributed to the same stpy-localized ^3IL_t excited state. Rise times of 4.5 ± 0.7 ps in CH_2Cl_2 and 4.1 ± 0.2 ps in acetonitrile were estimated for the 2027 cm^{-1} band. This kinetics can be identified with the 3.5 ps rise of the TA and TR^3 signals. The 2027 cm^{-1} band is most prominent at 10−15 ps. Then it decays, being replaced by another band at ca.2031 cm^{-1} (Figures 7b and 9). This conversion is fully completed between 50 and 100 ps. The 2031 cm^{-1} band then remains constant beyond 1 ns. Because of a close similarity with the $Re(stpy)_2$ system discussed above, it is attributed to a stpy-localized ^3IL_p state with a perpendicular geometry.

TRIR spectra in the region of stpy ν(C═C) vibrations exhibit a bleach at 1616 cm^{-1} which becomes fully developed at about 15−20 ps, supporting the delayed formation of an ^{3}IL state. No well-developed transient IR feature was observed. Weakness of the signal and overlapping broad background absorption prevented any quantitative analysis.

Discussion

UV excitation of the free stpy ligand populates a $^1\pi\pi^*$ and, probably, also $^1n\pi^*$ excited states[43] which decay with lifetimes of ca. 3 and 10 ps. Photoisomerization to the cis isomer occurs with a quantum yield of 0.37,[22] slightly smaller than that of *t*-stilbene (0.48).[63] The $^1\pi\pi^*$ lifetime of stpy is much shorter than that of *t*-stilbene (90 ± 5 ps) due to mixing between the $^1\pi\pi^*$ and $^1n\pi^*$ characters.[16] With respect to the following discussion, it is important to note that the trans−cis isomerization under direct irradiation of both stilbene and stpy occurs on singlet potential-energy surfaces. The triplet mechanism is possible if triplet sensitizers, such as benzophenone, are used. Quantum yields of 0.50 and 0.40 were reported for sensitized isomerization of *t*-stilbene and *t*-stpy, respectively.[22,63]

Information on the nature of the lowest allowed electronic transitions and, hence, the optically populated Franck−Condon states of $Re(stpy)_2$ and Re(stpy)(bpy) is provided by UV−vis absorption and resonance Raman spectra. The structured low-

SCHEME 1: Proposed Excited-State Behavior of $[Re(Cl)(CO)_3(stpy)_2]$[a]

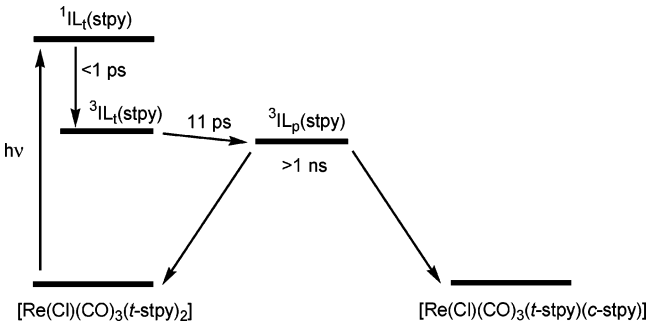

[a] Excited-state localization is shown in brackets

SCHEME 2: Proposed Excited-State Behavior of $[Re(stpy)(CO)_3(bpy)]^+$ [a]

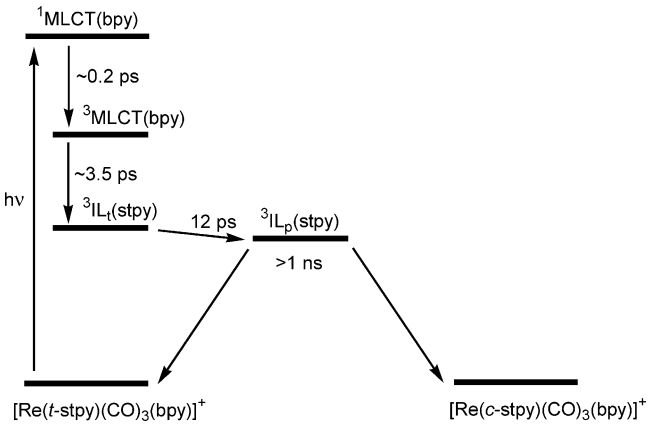

[a] Excited-state localization is shown in brackets

temperature UV absorption,[19] enhancement of Raman bands due to stpy vibrations, and absence of the intensity enhancement of the in-phase ν(CO) A′(1) Raman band show that the near-UV absorption spectrum of $Re(stpy)_2$ is dominated by stpy-localized $\pi\pi^*$ IL transitions. The Re → stpy MLCT transitions, if present, lie at higher energies. The situation is very similar for Re(bpy)(stpy), whose near-UV spectrum is also dominated by a stpy-localized $\pi\pi^*$ IL transition. However, observation of a weakly enhanced Raman band due to a bpy-localized vibration at 1494 cm^{-1} indicates the presence of a Re → bpy transition, which gives rise to an absorption tail between 390 and 420 nm. It follows that the 400 nm laser-pulse irradiation, used for the ultrafast studies, initially populates the ^1IL_t $\pi\pi^*$ state of $Re(stpy)_2$ and the ^{1}MLCT(bpy) state of Re(stpy)(bpy).

The proposed mechanisms of the excited-state behavior of the complexes $Re(stpy)_2$ and Re(stpy)(bpy) are shown in Schemes 1 and 2, respectively.

In the case of $Re(stpy)_2$ the optically prepared ^1IL_t state undergoes an ultrafast (≤ 0.9 ps) ISC to the corresponding triplet state ^3IL_t with the same trans geometry. The ^3IL_t excited state of $Re(stpy)_2$ is characterized by near-UV absorption below ~500 nm, resonantly enhanced Raman bands due to stpy-localized vibrations, and the characteristic[54−57] ν(CO) TRIR pattern. The excited-state ν(CO) IR bands are shifted to lower wavenumbers relative to the ground state (ca. −12 cm^{-1} for the highest A′(1) band) due to donation of electron density from the π^* stpy orbital, occupied in the ^3IL_t state, to d_π Re orbitals.[54]

The ^3IL_t state undergoes in a fluid solution an 11 ps conversion to another long-lived (≫1 ns) excited state, which is characterized by a much weaker absorption in the visible region, lack of resonantly enhanced Raman signal, and ν(CO) pattern that again points to its ^{3}IL character. The downshift of the A′(1) band from the ground-state position is relatively small (ca. −7 cm^{-1}), and the A′(2) and A″ bands are even shifted slightly upward, by ≤+8 cm^{-1}. We assign this species as an ^3IL_p excited state of the stpy ligand in which the pyridine and phenyl rings are oriented approximately perpendicularly to each other. The loss of π-delocalization in the perpendicular configuration accounts for the observed near-disappearance of absorption in the visible region and for the ν(CO) wavenumbers being slightly higher than those for the ^3IL_t state. The latter effect is caused by weakening of the π donation to the Re(CO)$_3$ unit. The ^3IL_p excited state is the immediate precursor of the trans−cis isomerization, which occurs for $Re(stpy)_2$ with a quantum yield of 0.49.[19] It is assumed that ^3IL_p undergoes a nanosecond ISC to the ground state in a perpendicular geometry, from which either the trans starting configuration is reformed or isomerization to the cis isomer is completed by further ~90° rotation.

Compared to free *t*-stilbene and stpy, it follows that coordination to a Re atom in $Re(stpy)_2$ switches the isomerization mechanism from singlet to triplet $\pi\pi^*$ potential-energy surfaces. This can be viewed as intramolecular triplet sensitization. The ^1IL_t → ^3IL_t ISC is a subpicosecond process, facilitated by the heavy-atom effect of the rhenium atom. The following ~90° rotation around the stpy C═C bond in the ^3IL_t state, to form the perpendicular intermediate ^3IL_p, is herein observed directly for the first time, and its time constant is determined as 11 ps in CH_2Cl_2. It does not occur in a rigid PMMA film. The lifetime of the perpendicular ^3IL_p excited state is in the nanosecond range, similar to the $^3\pi\pi^*$ state of *t*-stilbene.[17,21] Apparently the Re heavy-atom effect does not affect the ^3IL_p → GS ISC much, whose rate might be limited by geometrical constraints and shapes of the potential-energy surfaces.

Photochemistry of Re(stpy)(bpy) starts with population of a Re → bpy ^{3}MLCT excited state by ISC from the optically excited ^{1}MLCT state, which occurs with a time constant of ca. 0.2 ps. The ^{3}MLCT state is characterized by a typical TRIR spectral pattern with upshifted ν(CO) bands.[44,54,55,57−61] The ^{3}MLCT state is formed vibrationally hot, as documented by the broadness of the ν(CO) IR bands and their small dynamic shift

SCHEME 3: Schematic Orbital View of the ^{3}MLCT → ^3IL_t Conversion in $[Re(stpy)(CO)_3(bpy)]^+$

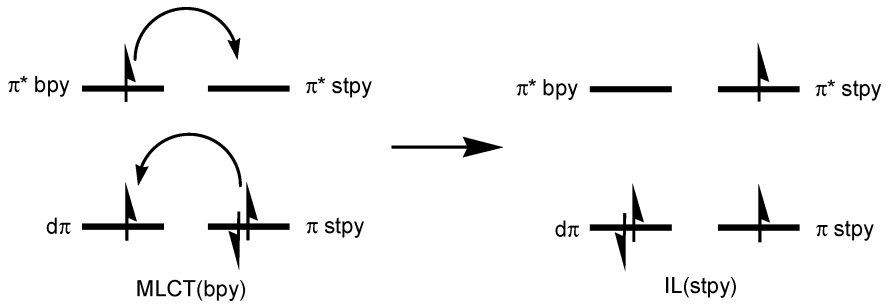

to higher wavenumbers.[61,62] The ^{3}MLCT state decays into a ^3IL_t state with a time constant of ~3.5 ps. UV−vis absorption, resonance Raman, and IR spectra of the ^3IL_t excited state of Re(stpy)(bpy) are very similar to those discussed above for Re(stpy)$_2$. All the ^3IL_t spectral features show rise times commensurate with the decay time of the ^{3}MLCT state. It should be noted that the $^3MLCT \rightarrow {}^3IL_t$ conversion involves a vibrationally hot ^{3}MLCT state since rates of conversion and vibrational cooling are comparable. The following $^3IL_t \rightarrow {}^3IL_p$ ~90° rotation around the stpy C═C bond occurs with a time constant of 12 ps. The spectroscopic characteristics of the ^3IL_p state are very similar to those of Re(stpy)$_2$. The ^3IL_p lifetime is in the nanosecond region, beyond the range of our experiment. This can be compared to the 28 ns decay that was determined for a ^{3}IL state of a similar complex [Re(bpe)(CO)$_3$(phen)]$^+$, for which a perpendicular bpe geometry was also postulated.[64] The ^3IL_p state is assumed to decay to the ground state while preserving the perpendicular geometry. Further backward or forward 90° rotation will form the trans or cis isomer, respectively. The isomerization quantum yield of Re(stpy)(bpy) was reported to be very low.[25] (A value of 0.21 was determined[26] for [Re(bpe)(CO)$_3$(bpy)]$^+$.) It can be limited either by inefficient ^3IL_t population from the ^{3}MLCT state or by asymmetric evolution on the ground-state surface. On the basis of comparison with analogous complexes, the ^{3}MLCT state of Re(stpy)(bpy) would be expected[34] to have a ca. 230 ns lifetime were the conversion to the ^3IL_t state absent. The 3.5 ps ^{3}MLCT lifetime found for Re(stpy)(bpy) essentially implies that the $^3MLCT \rightarrow {}^3IL_t$ conversion is complete.[65] Therefore, the isomerization quantum yield cannot be limited by a competitive relaxation of the ^{3}MLCT state to the ground state. Instead, it appears to be diminished by steric constraints in the low-symmetry Re(stpy)(bpy) molecule, which could make the ground-state potential-energy surface asymmetric with respect to the forward and backward rotation around the stpy C═C bond.

Coordination of isomerizable stpy ligand to a Re^I(CO)$_3$(bpy) moiety changes the isomerization pathway from the singlet to triplet $\pi\pi^*$ potential-energy surface in the same way discussed above for Re(stpy)$_2$. More interestingly, it was found that the stpy-localized ^3IL_t state is populated within a few picoseconds from a Re → bpy ^{3}MLCT excited state. The $^3MLCT \rightarrow {}^3IL_t$ conversion formally involves simultaneous population and depopulation of four orbitals of the Re^I(CO)$_3$(bpy) and *t*-stpy moieties, Scheme 3. This qualitative picture essentially amounts to an intramolecular energy transfer from the excited Re^I(CO)$_3$(bpy) chromophore to the axial *t*-stpy ligand via a Dexter mechanism. Electronic coupling between the two chromophores is provided by the d_π orbital, which overlaps with all relevant bpy and stpy orbitals. This coupling has to be relatively strong since the energy transfer in [Re(stpy)(CO)$_3$(bpy)]$^+$ is more than 6 orders of magnitude faster than the $^3MLCT \rightarrow {}^3\pi\pi^*$(stilbene) energy transfer in [Re(*t*-stilbene-C(═O)NHCH$_2$-4-pyridine)(CO)$_3$(bpy)]$^+$ (1.7 μs),[24] which can be assumed to take place with a comparable driving force and reorganization energy. Energy transfer in [Re(stpy)(CO)$_3$(bpy)]$^+$ is also much faster than that in polynuclear complexes containing stpy-like bridging ligand L [{Re(CO)$_3$(bpy)}$_n$(μ-L)]$^{n+}$ (n = 2 and 3)[28,29] or in [Re(R-pyridine)(CO)$_3$(bpy)]$^+$, where R is an energy acceptor (anthracene, CpM^{II}(arene), M = Fe, Ru).[66,67]

Conclusions

Coordination of a photoisomerizing stilbene-like ligand, *trans*-4-styrylpyridine, to a Re^I center in complexes *fac*-[Re(Cl)(CO)$_3$(stpy)$_2$] and *fac*-[Re(stpy)(CO)$_3$(bpy)]$^+$ switches the trans−cis isomerization mechanism from a spin singlet to a triplet $\pi\pi^*$ excited-state potential-energy surface. The Re^I moiety acts as an intramolecular triplet sensitizer, facilitating the $^1\pi\pi^* \rightarrow {}^3\pi\pi^*$ intersystem crossing to the femtosecond range.

An indirect population of the reactive intraligand $^3\pi\pi^*$ excited state by a picosecond internal conversion from a Re → bpy ^{3}MLCT excited state occurs in the case of *fac*-[Re(stpy)(CO)$_3$(bpy)]$^+$. This process amounts to an intramolecular energy transfer from a Re^I(CO)$_3$(bpy) chromophore to a stpy ligand.

The trans−cis isomerization of the stpy ligand is preceded by a ~90° rotation around the C═C bond, which occurs in an intraligand $^3\pi\pi$ excited state with a 11−12 ps time constant. An intraligand $^3\pi\pi$ excited state with a perpendicular orientation of the pyridine and phenyl rings is formed. The following intersystem crossing to the ground state, which leads to isomerization, is much slower, taking place in the nanosecond range. Intraligand rotation and, hence, isomerization is hindered by a rigid medium, as observed in a PMMA film.

Re → stpy MLCT excited states are not involved in the isomerization mechanism.

Acknowledgment. This research was funded by EPSRC, CCLRC, and COST Action D14. Dr. Ian P. Clark (Nanosecond Laboratory, CCLRC Rutherford Appleton Laboratory) and Mr. Michiel Groeneveld (Institute of Molecular Chemistry, University of Amsterdam) are thanked for their help in measuring stationary resonance Raman and time-resolved UV−vis spectra, respectively. Ms. Ana Maria Blanco Rodriguez is thanked for making and measuring the PMMA films. Fruitful and stimulating discussions with Dr. A. W. Parker (CCLRC Rutherford Appleton Laboratory) are gratefully appreciated.

References and Notes

(1) Hamaguchi, H.; Iwata, K. *Bull. Chem. Soc. Jpn.* **2002**, *75*, 883−897.
(2) Okamoto, H. *J. Phys. Chem. A* **1999**, *103*, 5852−5857.
(3) Takeuchi, S.; Tahara, T. *Chem. Phys. Lett.* **2000**, *326*, 430−438.
(4) Matousek, P.; Parker, A. W.; Toner, W. T.; Towrie, M.; de Faria, D. L. A.; Hester, R. E.; Moore, J. N. *Chem. Phys. Lett.* **1995**, *237*, 373−379.
(5) Iwata, K.; Ozawa, R.; Hamaguchi, H. *J. Phys. Chem. A* **2002**, *106*, 3614−3620.
(6) Han, W.-G.; Lovell, T.; Liu, T.; Noodleman, L. *ChemPhysChem* **2002**, *3*, 167−178.
(7) Gai, F.; Hasson, K. C.; McDonald, J. C.; Anfinrud, P. A. *Science* **1998**, *279*, 1886−1891.
(8) Wang, Q.; Schoenlein, R. W.; Peteanu, L. A.; Mathies, R. A.; Shank, C. V. *Science* **1994**, *266*, 422−424.
(9) Schoenlein, R. W.; Peteanu, L. A.; Mathies, R. A.; Shank, C. V. *Science* **1991**, *254*, 412−415.
(10) Gärtner, W. *Angew. Chem., Int. Ed.* **2001**, *40*, 2977−2981.
(11) Hellingwerf, K. J.; Hendriks, J.; Gensch, T. *J. Phys. Chem. A* **2003**, *107*, 1082−1094.
(12) Birge, R. R.; Parsons, B.; Song, Q. W.; Tallent, J. R. In *Molecular Electronics*; Jortner, J., Ratner, M., Eds.; Blackwell Science Ltd.: Oxford, 1997; pp 439−472.
(13) Görner, H.; Kuhn, H. J. In *Advances in Photochemistry*; Neckers, D. C., Volman, D. H., von Bünau, G., Eds.; J. Wiley & Sons: 1995; Vol. 19, p 1.
(14) Saltiel, J. *J. Am. Chem. Soc.* **1967**, *89*, 1036−1037.
(15) Orlandi, G.; Siebrand, W. *Chem. Phys. Lett.* **1975**, *30*, 352−354.
(16) Greene, B. I.; Hochstrasser, R. M.; Weisman, R. B. *Chem. Phys. Lett.* **1979**, *62*, 427−430.
(17) Görner, H.; Schulte-Frohlinde, D. *J. Phys. Chem.* **1981**, *85*, 1835−1841.
(18) Langkilde, F. W.; Wilbrandt, R.; Brouwer, A. M.; Negri, F.; Zerbetto, F.; Orlandi, G. *J. Phys. Chem.* **1994**, *98*, 2254−2265.
(19) Wrighton, M. S.; Morse, D. L.; Pdungsap, L. *J. Am. Chem. Soc.* **1975**, *97*, 2073−2079.
(20) Görner, H.; Schulte-Frohlinde, D. *J. Phys. Chem.* **1979**, *83*, 3107−3118.

(21) Lavilla, J. A.; Goodman, J. L. *Chem. Phys. Lett.* **1987**, *141*, 149−153.
(22) Whitten, D. G.; McCall, M. T. *J. Am. Chem. Soc.* **1969**, *91*, 5097−5103.
(23) Bartocci, G.; Bortolus, P.; Mazzucato, U. *J. Phys. Chem.* **1973**, *77*, 605−610.
(24) Schanze, K. S.; Lucia, L. A.; Cooper, M.; Walters, K. A.; Ji, H.-F.; Sabina, O. *J. Phys. Chem. A* **1998**, *102*, 5577−5584.
(25) Yam, V. W.-W.; Lau, V. C.-Y.; Wu, L.-X. *J. Chem. Soc., Dalton Trans.* **1998**, 1461−1468.
(26) Wenger, O. S.; Henling, L. M.; Day, M. W.; Winkler, J. R.; Gray, H. B. *Inorg. Chem.* **2004**, *43*, 2043−2048.
(27) Itokazu, M. K.; Polo, A. S.; de Faria, D. L. A.; Bignozzi, C. A.; Iha, N. Y. M. *Inorg. Chim. Acta* **2001**, *313*, 149−155.
(28) Sun, S.-S.; Lees, A. J. *Organometallics* **2002**, *21*, 39−49.
(29) Sun, S.-S.; Robson, E.; Dunwoody, N.; Silva, A. S.; Brinn, I. M.; Lees, A. J. *Chem. Commun.* **2000**, 201−202.
(30) Itokazu, M. K.; Polo, A. S.; Iha, N. Y. M. *J. Photochem. Photobiol., A: Chem.* **2003**, *160*, 27−32.
(31) Lewis, J. D.; Perutz, R. N.; Moore, J. N. *Chem. Commun.* **2000**, 1865−1866.
(32) Lewis, J. D.; Moore, J. N. *Dalton Trans.* **2004**, 1376−1385.
(33) Williams, J. L. R.; Adel, R. E.; Carlson, J. M.; Reynolds, G. A.; Borden, D. G.; Ford, J. A., Jr. *J. Org. Chem.* **1963**, *28*, 387−390.
(34) Hino, J. K.; Della Ciana, L.; Dressick, W. J.; Sullivan, B. P. *Inorg. Chem.* **1992**, *31*, 1072−1080.
(35) Vergeer, F. W.; Kleverlaan, C. J.; Stufkens, D. J. *Inorg. Chim. Acta* **2002**, *327*, 126−133.
(36) Vlček, A., Jr.; Farrell, I. R.; Liard, D. J.; Matousek, P.; Towrie, M.; Parker, A. W.; Grills, D. C.; George, M. W. *J. Chem. Soc., Dalton Trans.* **2002**, 701−712.
(37) Liard, D. J.; Busby, M.; Farrell, I. R.; Matousek, P.; Towrie, M.; Vlček, A., Jr. *J. Phys. Chem. A* **2004**, *108*, 556−567.
(38) Matousek, P.; Parker, A. W.; Taday, P. F.; Toner, W. T.; Towrie, M. *Opt. Commun.* **1996**, *127*, 307−312.
(39) Towrie, M.; Parker, A. W.; Shaikh, W.; Matousek, P. *Meas. Sci. Technol.* **1998**, *9*, 816−823.
(40) Matousek, P.; Towrie, M.; Stanley, A.; Parker, A. W. *Appl. Spectrosc.* **1999**, *53*, 1485−1489.
(41) Matousek, P.; Towrie, M.; Ma, C.; Kwok, W. M.; Phillips, D.; Toner, W. T.; Parker, A. W. *J. Raman Spectrosc.* **2001**, *32*, 983−988.
(42) Towrie, M.; Grills, D. C.; Dyer, J.; Weinstein, J. A.; Matousek, P.; Barton, R.; Bailey, P. D.; Subramaniam, N.; Kwok, W. M.; Ma, C. S.; Phillips, D.; Parker, A. W.; George, M. W. *Appl. Spectrosc.* **2003**, *57*, 367−380.
(43) Marconi, G.; Bartocci, G.; Mazzucato, U.; Spalletti, A.; Abbate, F.; Angeloni, L.; Castellucci, E. *Chem. Phys.* **1995**, *196*, 383−393.
(44) Busby, M.; Matousek, P.; Towrie, M.; Clark, I. P.; Motevalli, M.; Hartl, F.; Vlček, A., Jr. *Inorg. Chem.* **2004**, *43*, 4523−4530.
(45) Watanabe, H.; Okamoto, Y.; Furuya, K.; Sakamoto, A.; Tasum, M. *J. Phys. Chem. A* **2002**, *106*, 3318.
(46) van Slageren, J.; Klein, A.; Záliš, S.; Stufkens, D. J. *Coord. Chem. Rev.* **2001**, *219*−*221*, 937−955.
(47) Stufkens, D. J. *Coord. Chem. Rev.* **1990**, *104*, 39−112.
(48) Schoonover, J. R.; Chen, P.; Bates, W. D.; Dyer, R. B.; Meyer, T. J. *Inorg. Chem.* **1994**, *33*, 793−797.
(49) Smothers, W. K.; Wrighton, M. S. *J. Am. Chem. Soc.* **1983**, *105*, 1067−1069.
(50) Kovalenko, S. A.; Schanz, R.; Hennig, H.; Ernsting, N. P. *J. Chem. Phys.* **2001**, *115*, 3256−3273.
(51) Shida, T. *Physical Sciences Data 34. Electronic Absorption Spectra of Radical Ions*; Elsevier: Amsterdam-Oxford-New York-Tokyo, 1988.
(52) Weaver, W. L.; Huston, L. A.; Iwata, K.; Gustafson, T. L. *J. Phys. Chem.* **1992**, *96*, 8956−8961.
(53) Hester, R. E.; Matousek, P.; Moore, J. N.; Parker, A. W.; Toner, W. T.; Towrie, M. *Chem. Phys. Lett.* **1993**, *208*, 471−478.
(54) Dattelbaum, D. M.; Omberg, K. M.; Hay, P. J.; Gebhart, N. L.; Martin, R. L.; Schoonover, J. R.; Meyer, T. J. *J. Phys. Chem. A* **2004**, *108*, 3527−3536.
(55) Kuimova, M. K.; Alsindi, W. Z.; Dyer, J.; Grills, D. C.; Jina, O. S.; Matousek, P.; Parker, A. W.; Portius, P.; Sun, X.-Z.; Towrie, M.; Wilson, C.; Yang, J.; George, M. W. *Dalton Trans.* **2003**, 3996−4006.
(56) Schoonover, J. R.; Strouse, G. F.; Dyer, R. B.; Bates, W. D.; Chen, P.; Meyer, T. J. *Inorg. Chem.* **1996**, *35*, 273−274.
(57) Schoonover, J. R.; Strouse, G. F. *Chem. Rev.* **1998**, *98*, 1335−1355.
(58) Dattelbaum, D. M.; Martin, R. L.; Schoonover, J. R.; Meyer, T. J. *J. Phys. Chem. A* **2004**, *108*, 3518−3526.
(59) Gamelin, D. R.; George, M. W.; Glyn, P.; Grevels, F.-W.; Johnson, F. P. A.; Klotzbücher, W.; Morrison, S. L.; Russell, G.; Schaffner, K.; Turner, J. J. *Inorg. Chem.* **1994**, *33*, 3246−3250.
(60) George, M. W.; Johnson, F. P. A.; Westwell, J. R.; Hodges, P. M.; Turner, J. J. *J. Chem. Soc., Dalton Trans.* **1993**, 2977−2979.
(61) Liard, D. J.; Busby, M.; Matousek, P.; Towrie, M.; Vlček, A., Jr. *J. Phys. Chem. A* **2004**, *108*, 2363−2369.
(62) Asbury, J. B.; Wang, Y.; Lian, T. *Bull. Chem. Soc. Jpn.* **2002**, *75*, 973−983.
(63) Hammond, G. S.; Saltiel, J.; Lamola, A. A.; Turro, N. J.; Bradshaw, J. S.; Cowan, D. O.; Counsell, R. C.; Vogt, V.; Dalton, C. *J. Am. Chem. Soc.* **1964**, *86*, 3197−3217.
(64) Dattelbaum, D. M.; Itokazu, M. K.; Iha, N. Y. M.; Meyer, T. J. *J. Phys. Chem. A* **2003**, *107*, 4092−4095.
(65) The mechanism proposed herein excludes the possibility of a long-lived emission from Re(stpy)(bpy). Using a carefully purified sample, we saw no emission from a CH_3CN solution at ambient temperature using either a steady-state emission spectrometer or time-correlated single-photon counting, contrary to a previous report.[25]
(66) MacQueen, D. B.; Eyler, J. R.; Schanze, K. S. *J. Am. Chem. Soc.* **1992**, *114*, 1897−1898.
(67) Wang, Y.; Schanze, K. S. *Inorg. Chem.* **1994**, *33*, 1354−1362.